

Dynamics of metastable Standard Model particles from long-lived particle decays in the MeV primordial plasma

Kensuke Akita,^{1,*} Gideon Baur,^{2,3,†} Maksym Ovchynnikov,^{4,2,‡} Thomas Schwetz,^{2,§} and Vsevolod Syvolap^{5,¶}

¹*Department of Physics, The University of Tokyo, Bunkyo-ku, Tokyo 113-0033, Japan*

²*Institut für Astroteilchen Physik, Karlsruher Institut für Technologie (KIT), Hermann-von-Helmholtz-Platz 1, 76344 Eggenstein-Leopoldshafen, Germany*

³*Bethe Center for Theoretical Physics, Universität Bonn, D-53115, Germany*

⁴*Theoretical Physics Department, CERN, 1211 Geneva 23, Switzerland*

⁵*Instituut-Lorentz, Leiden University, Niels Bohrweg 2, 2333 CA Leiden, The Netherlands*

(Dated: November 5, 2024)

We investigate the cosmological impact of hypothetical unstable new physics particles that decay in the MeV-scale plasma of the Early Universe. Focusing on scenarios where the decays produce metastable species such as muons, pions, and kaons, we systematically analyze the dynamics of these particles using coupled Boltzmann equations governing their abundances. Our results demonstrate that the metastable species can efficiently annihilate or interact with nucleons, which often leads to their disappearance prior to decay. The suppression of decay significantly alters the properties of cosmic neutrinos, impacting cosmological observables like Big Bang nucleosynthesis and the Cosmic Microwave Background. To support further studies, we provide a public `Mathematica` code that traces the evolution of these metastable particles and apply it to several new physics models.

I. INTRODUCTION

The thermal plasma of the Early Universe near the epoch of neutrino decoupling, at temperatures $T \lesssim 5$ MeV [1], serves as a crucial window into potential new physics. Any new particles or interactions present during this period can leave imprints on primordial neutrinos, affecting their abundance and energy distribution. These modifications, in turn, influence key cosmological observables, including primordial nuclear abundances [2–8], the Cosmic Microwave Background (CMB) [5, 9–20], and the cosmological implications of neutrino mass [21–24].

One intriguing scenario involves the existence of hypothetical Long-Lived Particles (LLPs), X , with lifetimes $\tau_X \lesssim 1$ s. These particles can decay into Standard Model (SM) particles, such as neutrinos, nucleons, electromagnetic (EM) particles – e^\pm and photons, and various *metastable particles*

$$Y, \bar{Y} = \mu^\pm, \pi^\pm, K^\pm, K_L. \quad (1)$$

The specific decay channels determine how LLPs influence the neutrino population. A key quantity in this respect is the effective number of neutrino species N_{eff} . In the absence of other relativistic particles beyond the SM, N_{eff} is defined as the properly weighted ratio of neutrino and photon energy densities (see later for a precise definition). Decays into EM particles can heat the EM plasma, thereby reducing N_{eff} . On the other hand, decays into neutrinos have effects that depend on the energy of the injected neutrinos, E_ν , relative to the thermal

neutrino energy $\sim 3T$. If $E_\nu \simeq 3T$, decays heat the neutrino plasma, which leads to an increase of N_{eff} without substantial neutrino spectral distortions [25]. However, if $E_\nu \gg 3T$, N_{eff} can also decrease because of non-trivial effects related to non-thermal distortions of the neutrino momentum distributions [18, 20, 26, 27].

Examples of LLPs that decay into Y particles include Higgs-like scalars [28], generic pseudoscalars such as axion-like particles with various coupling schemes [29–33], particles coupled to quark currents like dark photons and $B - L$ mediators [34], Heavy Neutral Leptons [35], and neutralinos.

The metastable particles Y may subsequently decay into neutrinos and EM particles. As the decay of these Y particles is governed by weak interactions, their inverse lifetimes are relatively low, $\tau_Y^{-1} \sim (10^6 - 10^8) \text{s}^{-1}$, exceeding the characteristic interaction rates of Y with the primordial plasma. Consequently, Y particles can engage in various processes before decaying. For charged Y particles, frequent interactions with electrons and photons can transfer their kinetic energy to the EM plasma [4, 14, 36, 37]. This was incorporated in the studies [14, 15, 17, 18, 20, 38], which examined the impact of LLP decays into Y particles on neutrino properties. These works generally assumed that Y particles inevitably decay (in the case of charged Y , this happens after thermalizing their kinetic energy with the SM plasma).

In this paper, we highlight critical aspects of Y particle dynamics that have been overlooked. Specifically, before decaying, they can undergo processes that lead to their disappearance without producing neutrinos. These processes include annihilations $Y + \bar{Y} \rightarrow \text{SM}$, where \bar{Y} is similarly produced by the decaying LLP, and inter-

* kensuke@hep-th.phys.s.u-tokyo.ac.jp

† gbaur@uni-bonn.de

‡ maksym.ovchynnikov@cern.ch

§ schwetz@kit.edu

¶ v.syvolap@umail.leidenuniv.nl

actions with nucleons $Y + \mathcal{N} \rightarrow \mathcal{N}' + \text{SM}$.¹ Although the instant abundances of Y , \bar{Y} , and nucleons are small, the large interaction cross-sections mediated by strong or electromagnetic forces render these processes highly efficient. Depending on the temperature, their rates can compete or even exceed the decay rate, potentially preventing any neutrino injection. Consequently, the properties of cosmic neutrinos are significantly altered compared to scenarios where Y decays are inevitable. In particular, within the lifetime range $0.01 \text{ s} \lesssim \tau_X \lesssim 10 \text{ s}$, the effective number of relativistic degrees of freedom N_{eff} and the degree of neutrino spectral distortions are substantially reduced, while in presence of the charged kaons the energy distributions of neutrinos and antineutrinos may become asymmetric.

The paper is organized as follows. In Sec. II, we describe the properties of the metastable particles Y and their interactions in the primordial plasma. Sec. III outlines the general approach used to study the coupled dynamics of Y particles and nucleon densities. Sec. IV presents a simplified analysis for the cases of muons and charged pions, illustrating the extent to which decay probabilities are suppressed based on the temperature range of Y injection. Sec. V offers a general discussion on how Y dynamics impact neutrino properties, including N_{eff} , the neutrino distribution function, and the neutrino-antineutrino energy asymmetry. Sec. VI explores the implications of Y disappearance on the evolution of various hypothetical LLPs, such as Higgs-like scalars and Heavy Neutral Leptons. Finally, Sec. VII summarizes our findings.

II. INTERACTIONS OF METASTABLE PARTICLES IN THE PRIMORDIAL MEV PLASMA

A brief summary of the properties and interactions of the Y particles is listed in Table I, while the relevant interaction diagrams are shown in Fig. 1.

We take the information about the decay modes from PDG [40], the interaction with nucleons from Ref. [36], and the results of this section for the annihilation channels. Below, we describe them in detail for each of the particles.

A. Muons

The muon lifetime is $\tau_\mu \approx 1.2 \cdot 10^{-6} \text{ s}$ – the largest among all the metastable particles. The only relevant

decay mode is into $e\nu_e\bar{\nu}_\mu$. The neutrino decay products may have energies as large as $E_\nu \approx m_\mu/2 \simeq 50 \text{ MeV}$, which well exceeds the thermal neutrino energies at MeV temperatures.

The energy loss processes are

$$\mu + \gamma \rightarrow \mu + \gamma \quad \text{and} \quad \mu + e \rightarrow \mu + e \quad (2)$$

The overall rate has the scaling

$$\Gamma_{\text{loss}} = \langle \sigma_{\text{loss}}^\mu v \rangle n_{\text{EM}} \sim \frac{\alpha_{\text{EM}}^2}{m_\mu E_{\text{thermal}}} T_{\text{EM}}^3, \quad (3)$$

where $E_{\text{thermal}} \approx 3T$ is the mean energy of thermal particles. At $T = 1 - 5 \text{ MeV}$, the rate is more than 9 orders of magnitude larger than the decay rate $\Gamma_{\text{decay}}^\mu = \hbar/\tau_\mu$. Because of this, we will assume that the muons are effectively at rest. The same conclusion holds for any other charged Y .

The annihilation processes are

$$\mu^+ + \mu^- \rightarrow e^+ + e^- \quad \text{and} \quad \mu^+ + \mu^- \rightarrow 2\gamma \quad (4)$$

They are thresholdless, and given that $m_\mu \gg m_e$, the thermal average $\langle \sigma v \rangle$ closely matches the zero-momentum cross-section:

$$\langle \sigma_{\text{ann}}^\mu v \rangle \approx \sum_{i=e,2\gamma} (\sigma_{\text{ann}}^{\mu \rightarrow i} v)_{i,p=0} \approx \frac{4\pi\alpha_{\text{EM}}^2}{m_\mu^2} \quad (5)$$

The annihilation rate $\Gamma_{\text{ann}}^\mu = \langle \sigma_{\text{ann}}^\mu v \rangle n_{\bar{\mu}}$ is also suppressed compared to the energy loss rate: the cross-section itself is smaller than energy loss one by the ratio $m_\mu/E_{\text{thermal}} \gg 1$, and the number density $n_{\bar{\mu}}$ of anti-muons (produced together with the muons) is much smaller than the thermal densities. This is because the instant \bar{Y} number density, entering the annihilation rate $\Gamma_{\text{ann}} = n_{\bar{Y}} \langle \sigma v \rangle$, is principally bounded from above by what can be accumulated before decays. It is $n_{\bar{Y}} \lesssim n_X \frac{\tau_Y}{\tau_X} \ll n_X$ (see a discussion in Sec. IV), and hence is much smaller than the available X number density (which is itself typically much smaller than the thermal number density). Note that generically, we assume that the same amounts of Y and \bar{Y} particles are produced by the X decays, and the above argument on the annihilation rate applies equally to the charge-conjugated case.

Muons interact with nucleons $\mathcal{N} = n, p$ by

$$\begin{aligned} \mu^- + p &\rightarrow n + \nu_\mu, \\ \mu^+ + n &\rightarrow p + \bar{\nu}_\mu. \end{aligned} \quad (6)$$

They are mediated by the weak force, which, together with the tiny amount of nucleons, makes the processes irrelevant [14, 37].

B. Charged pions

The lifetime of the charged pion is $\tau_\pi = 2.6 \cdot 10^{-8} \text{ s}$, 2 orders of magnitude smaller than for the muon. The

¹ The meson-driven $p \leftrightarrow n$ processes have been included in the works [4, 7, 8, 16, 36, 37, 39], studying the impact of various scenarios with LLPs decaying into Y s on primordial nuclear abundances. However, to the best of our knowledge, they have not been included in any previous study of the impact on neutrinos.

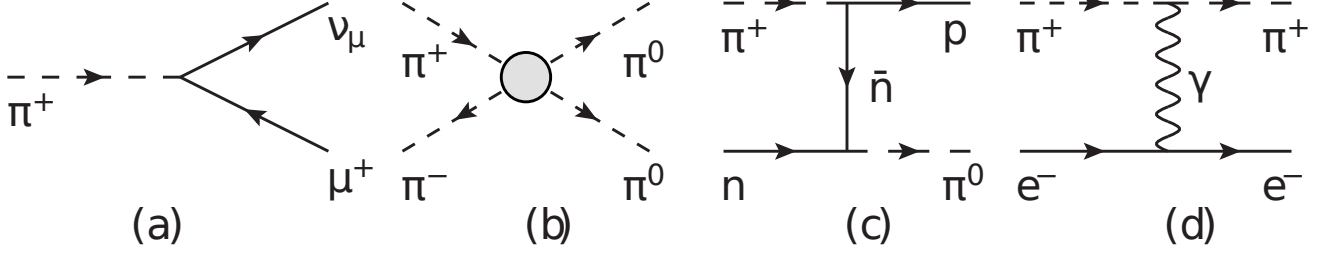


FIG. 1. Diagrams of different interaction processes with metastable particles Y in the primordial plasma: decay (a), annihilation $Y + \bar{Y} \rightarrow \text{SM}$ (b), the interaction with nucleons (c), and the elastic EM scattering that leads to the deposition of the Y 's kinetic energy in the EM plasma (d). Processes with the pion π^+ are considered as an example. The impact of the scattering off nucleons and annihilation process is demonstrated in Figs. 2-7.

Particle	Decays	Annihilations	Nucleon interactions
μ^\pm	$\tau = 2.2 \cdot 10^{-6} \text{ s}$ $e^\pm \nu_e^{(-)} \nu_\mu^{(-)} (100\%)$	$\langle \sigma\beta \rangle \approx 6 \cdot 10^{-2} \text{ GeV}^{-2}$ $\gamma\gamma (25\%)$ $e^+e^- (75\%)$	$\mu^-p \rightarrow n\nu_\mu$ $\mu^+n \rightarrow p\bar{\nu}_\mu$ Subdominant
π^\pm	$\tau = 2.6 \cdot 10^{-8} \text{ s}$ $\mu^\pm \nu_\mu^{(-)} : 100\%$	$\langle \sigma\beta \rangle \approx 3 - 5 \text{ GeV}^{-2}$ $2\pi^0 (\approx 100\%)$	$\pi^-p \rightarrow nX$ $\langle \sigma\beta \rangle \approx 4 - 4.6 \text{ GeV}^{-2}$ $\pi^+n \rightarrow pX$ $\langle \sigma\beta \rangle \approx 4 \text{ GeV}^{-2}$
K^\pm	$\tau = 1.23 \cdot 10^{-8} \text{ s}$ $\mu\bar{\nu}_\mu (63\%)$ $\pi^0 l \bar{\nu}_l (8.4\%)$ $\pi^+\pi^0 (20.7\%)$ $3\pi (7.4\%)$	$\langle \sigma\beta \rangle \approx 44 \text{ GeV}^{-2}$ $\pi^+\pi^- (66.6\%)$ $2\pi^0 (33.3\%)$	$K^-p \rightarrow \mathcal{N}2\pi$ $\langle \sigma\beta \rangle \approx 150 \text{ GeV}^{-2}$ $K^-n \rightarrow \mathcal{N}2\pi$ $\langle \sigma\beta \rangle \approx 10^2 \text{ GeV}^{-2}$
K_L	$\tau = 5.116 \cdot 10^{-8} \text{ s}$ $\pi^\pm l^\mp \nu_l (67.6\%)$ $3\pi (30.6\%)$	Same as K^\pm	$K_L p \rightarrow \mathcal{N}2\pi$ $\langle \sigma\beta \rangle \approx 42.5 \text{ GeV}^{-2}$ $K_L n \rightarrow \mathcal{N}2\pi$ $\langle \sigma\beta \rangle \approx 42.5 \text{ GeV}^{-2}$
K_S	$\tau = 0.89 \cdot 10^{-10} \text{ s}$ $2\pi^0 (30.7\%)$ $\pi^+\pi^- (69.2\%)$	Same as K^\pm	Same as K_L

TABLE I. Properties of the metastable particles in the primordial plasma. The meaning of the columns is as follows: the particle, its lifetime and decay modes, annihilation modes with their corresponding thermal-averaged cross-sections, and the same for the interactions with nucleons $\mathcal{N} = n, p$. For the thermal-averaged cross-sections, we provide the values at $T = 3 \text{ MeV}$.

main decay mode is

$$\pi^+ \rightarrow \mu^+ + \nu_\mu \quad (7)$$

The neutrino produced by decays of the pion at rest has a monochromatic energy $E_\nu = (m_\pi^2 - m_\mu^2)/2m_\pi \approx 29.8 \text{ MeV}$, which still greatly exceed thermal neutrino energies. The pion's energy loss rate is similar to the muon's one, being many orders of magnitude larger than the decay rate. As decaying pions inject muons, the evolution of π s and μ s is coupled.

Despite the much smaller lifetime, the processes of the annihilation and the interaction with nucleons are important for the pions: the corresponding processes are driven by the strong force, which means a much larger

cross-section. The dominant annihilation process is²

$$\pi^+ + \pi^- \rightarrow 2\pi^0. \quad (8)$$

It is close to the kinematic threshold, and the kinetic energy distribution of pions makes a non-negligible contribution to the cross-section. To compute it, we use the ChPT Lagrangian as implemented in [33], and then average over thermally distributed pion energies using [25, eq. (A.68)]. Before averaging over energies, we find

$$\sigma_{\text{ann}}^{2\pi^0} \beta = \frac{(10m_{\pi^+}^2 + 12p^2 - m_{\pi^0}^2)^2 \sqrt{m_{\pi^+}^2 - m_{\pi^0}^2 + p^2}}{576\pi f_\pi^4 (m_\pi^2 + p^2)^{\frac{3}{2}}}, \quad (9)$$

² The EM process, $\pi^+ + \pi^- \rightarrow 2\gamma$, although being far from the kinematic threshold, is suppressed by two orders of magnitude.

where p is the momentum of the interacting pion in the center-of-mass frame and $f_\pi \approx 93$ MeV is the pion decay constant. The thermal averaging increases the cross-section by a factor of 2 compared to the zero-momentum limit in the temperature range $T < 5$ MeV.

Let us now discuss interactions with nucleons. Since the pions are almost stopped, the most efficient processes are thresholdless. Those are [36]

$$\pi^- + p \rightarrow n + \pi^0/\gamma, \quad \pi^+ + n \rightarrow p + \pi^0/\gamma. \quad (10)$$

The thermal cross-sections behave as

$$\langle \sigma_{p \rightarrow n}^{\pi^-} \beta \rangle \approx 3.68 \cdot F_c^\pi(T) \text{ GeV}^{-2}, \quad (11)$$

$$\langle \sigma_{n \rightarrow p}^{\pi^+} \beta \rangle \approx 1.1 \langle \sigma_{p \rightarrow n}^{\pi^-} v \rangle / F_c^\pi(T), \quad (12)$$

Here,

$$F_c^X(T) = \frac{y_X}{1 - \exp[-y_X]}, \quad y_X = 2\pi\alpha_{\text{EM}}/v_{\text{rel},pX}, \quad (13)$$

is the Sommerfeld enhancement, occurring because of the formation of a quasi-bound state of the oppositely charged X and p particles with the relative velocity $v_{\text{rel},pX} = |\mathbf{v}_p - \mathbf{v}_X|$.

The resulting $\langle \sigma_{p \leftrightarrow n}^{\pi^\pm} \beta \rangle$ is comparable to $\langle \sigma_{\text{ann}}^{\pi^\pm} \beta \rangle$.

C. Kaons

The case of kaons is more complicated. There are four different kaons, K^\pm, K_L, K_S , with K_L/S being admixtures of K^0 and \bar{K}^0 . The lifetimes are $\tau_{K^\pm} \approx 1.23 \cdot 10^{-8}$ s, $\tau_{K_L} \approx 5.1 \cdot 10^{-8}$ s, and $\tau_{K_S} \approx 0.9 \cdot 10^{-10}$ s. All of them, except for K_S , have decay modes containing neutrinos. K_S decays into a pair of pions; its lifetime is very small, and it does not have time to participate in any other interactions before decaying. The neutrino energy may be as large as $m_K/2$.

K_L s do not lose their kinetic energy before participating in any further interaction. Here and below, we will treat them as particles-at-rest for simplicity.³

The dominant kaon annihilation processes are

$$K^+ + K^- \rightarrow \pi^+ + \pi^-, \quad K^+ + K^- \rightarrow 2\pi^0 \quad (14)$$

(and the same for K_L, K_S particles). Since $m_K - m_\pi \gg 3T$, the reactions are far from threshold, and we may

³ If including the finite energy distribution of kaons, the decay probability decreases with the γ factor (due to time dilation). On the other hand, the probabilities of the other processes would generically increase, as we enlarge the available scattering phase space. Therefore, our approximation would overestimate the decay probability of K_L . However, as we study GeV-scale LLPs, the impact of these changes would not be significant, which justifies the approach.

safely approximate their cross-sections σv by the zero-momentum result:

$$\langle \sigma_{\text{ann}}^K \beta \rangle \approx \frac{\sqrt{m_K^2 - m_\pi^2} (m_d(10m_K^2 + m_\pi^2) + m_\pi^2 m_s)^2}{3072\pi f_\pi^4 m_d^2 m_K^3}, \quad (15)$$

with the numeric value $\approx 44 \text{ GeV}^{-2}$. It is a factor of 10 larger than $\langle \sigma_{\text{ann}}^{\pi^\pm} \beta \rangle$, because the reaction is far from the threshold.

The interaction processes with nucleons \mathcal{N} are much more complicated than in the pion case. The thresholdless processes exist only for K_L, K^- , and go via the intermediate Λ/Σ resonances [36, 37]:

$$K^- + \mathcal{N} \rightarrow \Lambda/\Sigma + \pi \rightarrow \mathcal{N}' + 2\pi, \quad (16)$$

$$K_L + \mathcal{N} \rightarrow \Lambda/\Sigma + \pi \rightarrow \mathcal{N}' + 2\pi. \quad (17)$$

The absence of such processes for K^+ follows from the fact that they would require resonances with positive baryon number and strangeness, that do not exist. The asymmetry in the evolution of K^+, K^- induces an asymmetry in the energy distributions of neutrinos and antineutrinos; we will return to this phenomenon in Sec. VB.

The thermal cross-sections (here assuming that K_L is at rest) are [36]

$$\langle \sigma_{p \rightarrow n}^{K^-} \beta \rangle \approx 79 F_c^K(T) \text{ GeV}^{-2}, \quad \langle \sigma_{n \rightarrow p}^{K^-} \beta \rangle \approx 66 \text{ GeV}^{-2}, \quad (18)$$

$$\langle \sigma_{p \rightarrow p}^{K^-} \beta \rangle \approx 37 F_c^K(T) \text{ GeV}^{-2}, \quad \langle \sigma_{n \rightarrow n}^{K^-} \beta \rangle \approx 88 \text{ GeV}^{-2}, \quad (19)$$

$$\langle \sigma_{p \rightarrow n}^{K_L} \beta \rangle \approx 18 \text{ GeV}^{-2}, \quad \langle \sigma_{n \rightarrow p}^{K_L} \beta \rangle \approx 18 \text{ GeV}^{-2}. \quad (20)$$

Here, F_c is given by eq. (13).

Kaon decays, annihilations, and interaction with nucleons inject charged pions and/or muons, which do not transfer all their energy to the EM plasma. Therefore, the evolution of $K, \mu,$ and π populations is coupled.

III. DYNAMICS OF METASTABLE PARTICLES

In this section, we discuss our approach to studying the evolution of the Y particles in the primordial plasma. We assume a generic scenario when these metastable particles are injected by decays of some hypothetical LLP denoted by X at MeV temperatures. We are agnostic about the origin of X and parameterize its number density as

$$n_X = n_{X,0} \left(\frac{a(t_0)}{a(t)} \right)^3 \exp \left[-\frac{t - t_0}{\tau_X} \right] \quad (21)$$

Here, $n_{X,0}$ is the number density at some initial time t_0 , and τ_X is its lifetime.

Decays into Y s are only possible if $m_X > m_Y \gg 3T$. This means that the LLPs we consider have to be out-of-equilibrium at the temperatures of interest; otherwise,

their abundance would be exponentially suppressed. As for the LLP lifetimes, our main interest is in the range $\mathcal{O}(0.01 - 10)$ s. On the one hand, it covers the temperatures from the beginning of the neutrino decoupling to shortly after (in Λ CDM scenario). On the other hand, this is also the temperature range where the metastable particles may prefer to disappear without decaying.

In general, $n_{X,0}$ is an independent parameter, but for particular models with only two parameters – mass m_X and τ_X , it may be uniquely fixed due to the interactions of X with the SM, $n_{X,0} = n_{X,0}(m_X, \tau_X)$.

In order to study the dynamics of the metastable particles and neutrinos, we follow a two-step approach. First, we trace the evolution of Y particles in the expanding Universe. For the thermodynamics of the Universe, we use integrated Boltzmann equations [25]; when calculating the source terms for neutrinos and the EM particles, we, for simplicity, assume that all energy injection from Y decays goes to the EM plasma. Second, knowing the dynamics of the metastable particles, we use it as an input for the Boltzmann equations in the momentum space governing the evolution of neutrinos. For the latter, we use the modified code from [41] (its detailed description may be found in [42]).

This factorization is meaningful because an exact description of the evolution of neutrinos and EM plasma is not required for knowing the dynamics of Y s: it is mainly sensitive to the scale factor, which is determined by the overall energy density of the Universe. However, there is a possible mismatch in the time-temperature dynamics between the integrated and the unintegrated approaches. To minimize it, we provide the Y evolution input in terms of temperature and then utilize the time-temperature relation within the unintegrated approach.

A. System of equations

Let us now construct the system of equations for the Y abundances. Most of the Y s are charged and, therefore, effectively at rest; given this, it is adequate to consider the system of coupled integrated Boltzmann equations on their number densities.

As we have discussed in Sec. II, we have to solve the system for all Y s simultaneously, given that their dynamics are coupled: heavier Y s produce lighter ones because of decay, annihilation, or interactions with nucleons. Then, the resulting equations for the given Y and its antiparticle \bar{Y} take the form

$$\begin{cases} \frac{dn_Y}{dt} + 3Hn_Y = \frac{n_X}{\tau_X} N_Y^X - \frac{n_Y}{\tau_Y} - n_Y n_{\bar{Y}} \langle \sigma_{\text{ann}}^Y v \rangle + \left(\frac{dn_Y}{dt} \right)_{\mathcal{N}} + \sum_{Y' \neq Y} n_{Y'} \Gamma_{Y' \rightarrow Y}, \\ \frac{dn_{\bar{Y}}}{dt} + 3Hn_{\bar{Y}} = \frac{n_X}{\tau_X} N_{\bar{Y}}^X - \frac{n_{\bar{Y}}}{\tau_Y} - n_{\bar{Y}} n_Y \langle \sigma_{\text{ann}}^Y v \rangle + \left(\frac{dn_{\bar{Y}}}{dt} \right)_{\mathcal{N}} + \sum_{Y' \neq Y} n_{Y'} \Gamma_{Y' \rightarrow \bar{Y}}. \end{cases} \quad (22)$$

The meaning of the terms is as follows.

- The second term on the left-hand side appears due to the expansion of the Universe. $H = \sqrt{8\pi\rho/(3m_{\text{Pl}})}$ is the Hubble parameter, with the Planck mass $m_{\text{Pl}} = 1.2 \times 10^{19}$ GeV and the energy density of the Universe ρ .
- $\frac{n_X}{\tau_X} N_Y^X$ is the injection from decays of X . Apart from direct decays, we also include secondary contributions $X \rightarrow Z \rightarrow Y$, where Z are ultra short-lived particles with $\tau_Z \ll 10^{-8}$ s: $K_S, \rho^0, \eta, \omega$, etc. $N_Y^X = \sum_i \text{Br}_i \cdot N_Y^i$ is the amount of Y per X decay, with Br_i being the branching ratio of the given decay channel i , and N_Y^i denoting the number of Y s produced per this channel.
- The 2nd and 3rd terms on the r.h.s. of eq. (22) describe direct decays and annihilations of Y , respectively.
- $\left(\frac{dn_{Y/\bar{Y}}}{dt} \right)_{\mathcal{N}}$ is the evolution due to the interaction with nucleons $\mathcal{N} = p, n$:

$$\left(\frac{dn_{Y/\bar{Y}}}{dt} \right)_{\mathcal{N}} = -n_{Y/\bar{Y}} \sum_{\mathcal{N}} n_{\mathcal{N}} \langle \sigma_{\mathcal{N}}^{Y/\bar{Y}} v \rangle. \quad (23)$$

The interaction processes include the $p \leftrightarrow n$ conversion as well as the processes that do not change the N type.

- The summand $\sum_{Y' \neq Y} n_{Y'} \Gamma_{Y' \rightarrow Y}$ takes into account decay, annihilation, and nucleon interaction processes involving the metastable particles $Y' \neq Y$ with $m_{Y'} > m_Y$:

$$\Gamma_{Y' \rightarrow Y} = \frac{1}{\tau_{Y'}} N_Y^{Y', \text{decay}} + n_{\bar{Y}} \langle \sigma_{\text{ann}}^{Y'} v \rangle N_Y^{Y', \text{ann}} + \sum_{\mathcal{N}} n_{\mathcal{N}} \langle \sigma_{\mathcal{N}}^{Y'} v \rangle N_Y^{Y', \mathcal{N}}, \quad (24)$$

with $N_Y^{Y', \text{decay}}, N_Y^{Y', \text{ann}}, N_Y^{Y', \mathcal{N}}$ being the amounts of Y produced per given process. We calculate them using [40] for decays, [36] for the interaction with nucleons, and this work for the annihilation.

The system (22) has to be supplemented by the equations governing the evolution of EM and neutrino populations, the scale factor, and the nucleon number densities. The first we take from [25]. This determines the dynamics of the X 's number density (21) and the baryon-

to-photon ratio

$$\eta_B(T) = \eta_{B,\text{Planck}} \cdot \left(\frac{a(T_{\text{CMB}})T_{\text{CMB}}}{aT} \right)^3, \quad (25)$$

where $\eta_{B,\text{Planck}} = 7.06 \cdot 10^{-10}$ is fixed by the CMB measurements performed with Planck [43].

For the nucleon number density, we start with the definition

$$n_{\mathcal{N}}(t) \equiv n_B(t)X_{\mathcal{N}}(t) = n_\gamma \eta_B(t) \cdot X_{\mathcal{N}}(t), \quad (26)$$

where n_B is the baryon number density, and $X_{\mathcal{N}} \equiv n_{\mathcal{N}}/n_B$ is the relative fraction of the given nucleon ($X_n + X_p = 1$). The latter obeys the equation

$$\begin{aligned} \frac{dX_n}{dt} = & -X_n \left(\Gamma_{n \leftrightarrow p}^{\nu,e} + \sum_{y=Y,\bar{Y}} n_y \langle \sigma_{n \rightarrow p}^y v \rangle \right) + \\ & + (1 - X_n) \left(\Gamma_{p \rightarrow n}^{\nu,e} + \sum_{y=Y,\bar{Y}} n_y \langle \sigma_{p \rightarrow n}^y v \rangle \right), \end{aligned} \quad (27)$$

where $\Gamma_{n \leftrightarrow p}^{\nu,e}$ are rates of the weak conversion processes with neutrinos and electrons, while $n_y \langle \sigma_{p \leftrightarrow n}^y v \rangle$ are those driven by the Y particle. The latter processes are part of the total nucleon interaction rates $\langle \sigma_{\mathcal{N}}^Y v \rangle$:

$$\langle \sigma_{\mathcal{N}}^Y v \rangle = \langle \sigma_{\mathcal{N} \rightarrow \mathcal{N}}^Y v \rangle + \langle \sigma_{\mathcal{N} \rightarrow \mathcal{N}'}^Y v \rangle. \quad (28)$$

If Y is a meson, it completely dominates the evolution of X_n until the instant Y population is suppressed by many orders of magnitude compared to the neutrino number density [8]. This is because of the two factors. First, the meson-driven conversion cross-section is 16 orders of magnitude larger than the cross-section of the weak conversion. Second, at MeV temperatures, the probability of Y 's interaction with nucleons is comparable with its decay probability, so there is no a priori suppression. Therefore, in practice, the weak $p \leftrightarrow n$ conversion rates may be dropped from eq. (27).

The solution for X_n may be obtained by setting the right-hand-side of eq. (27) to zero (the so-called dynamic equilibrium):⁴

$$X_n \approx \frac{\sum_y n_y \langle \sigma_{p \rightarrow n}^y v \rangle}{\sum_y n_y \langle \sigma_{p \rightarrow n}^y v \rangle + \sum_y n_y \langle \sigma_{n \rightarrow p}^y v \rangle}. \quad (29)$$

Once we solve the coupled system of equations for μ, π, K, X_n , we may compute time-dependent probabilities to decay and disappear by annihilating or interacting

with nucleons:

$$P_{\text{decay}}^Y(t) = \frac{\tau_Y^{-1}}{\tau_Y^{-1} + \sum_{\mathcal{N}} n_{\mathcal{N}} \langle \sigma_{\mathcal{N}}^Y v \rangle + n_{\bar{Y}} \langle \sigma_{\text{ann}}^Y v \rangle}, \quad (30)$$

$$P_{\text{ann}}^Y(t) = \frac{n_{\bar{Y}} \langle \sigma_{\text{ann}}^Y v \rangle}{\tau_Y^{-1} + \sum_{\mathcal{N}} n_{\mathcal{N}} \langle \sigma_{\mathcal{N}}^Y v \rangle + n_{\bar{Y}} \langle \sigma_{\text{ann}}^Y v \rangle}, \quad (31)$$

$$P_{\mathcal{N}}^Y(t) = \frac{\sum_{\mathcal{N}} n_{\mathcal{N}} \langle \sigma_{\mathcal{N}}^Y v \rangle}{\tau_Y^{-1} + \sum_{\mathcal{N}} n_{\mathcal{N}} \langle \sigma_{\mathcal{N}}^Y v \rangle + n_{\bar{Y}} \langle \sigma_{\text{ann}}^Y v \rangle} \quad (32)$$

These probabilities serve as an input to calculate the impact on the neutrino and EM populations of the primordial plasma. We separate annihilations and interactions with nucleons, as the latter are very important for studying the impact of Y on BBN.

Assuming that we have computed the decay probability $P_{\text{decay}}^Y(t)$, the number density of Y s available for decays is again given by the dynamical equilibrium:

$$n_Y(t) = n_X(t) N_Y^X \frac{\tau_Y}{\tau_X} P_{\text{decay}}^Y(t) \quad (33)$$

We provide the implementation of this system and its solution for generic LLPs in a `Mathematica` code.⁵ Details on the code may be found in Appendix A.

IV. SIMPLE ESTIMATES OF Y EVOLUTION

Let us make a simplified analysis that allows us to understand the impact of annihilation and interaction with nucleons. First, let us neglect the influence of X particles on the Hubble expansion rate. Then, we may use the standard formula $a(t) \propto \sqrt{t}$ and $H(t) = \dot{a}/a = 1/2t$ for the radiation-dominated Universe, as well as the standard cosmological value for the baryon-to-photon ratio $\eta_B(1 \text{ MeV}) \approx 1.7 \cdot 10^{-9}$. Next, let us assume that various Y s evolve independently from each other. With all these approximations, we can still qualitatively describe the dynamics of the populations of Y and its antiparticle \bar{Y} , while presenting results in a simple form.

Similarly to the case of X_n , we may solve the system (22) analytically in the regime of dynamic equilibrium, when all the processes are much faster than the Hubble expansion.⁶ Assuming $n_Y = n_{\bar{Y}}$, we get

$$n_Y = \frac{\sqrt{\frac{4n_X \langle \sigma_{\text{ann}}^Y v \rangle}{\tau_X} + (\Gamma_{\mathcal{N}} + \tau_Y^{-1})^2} - \Gamma_{\mathcal{N}} - \tau_Y^{-1}}{2 \langle \sigma_{\text{ann}}^Y v \rangle}, \quad (34)$$

⁴ We have validated the dynamical equilibrium solutions for X_n and n_Y (eq. (33)) by computing first the exact solutions and comparing them with the approximate solution given by the dynamic equilibrium.

⁵ Available on [GitHub/maksymovchynnikov/Metastable-dynamics](https://github.com/maksymovchynnikov/Metastable-dynamics) and [10.5281/zenodo.14020343](https://zenodo.org/record/14020343).

⁶ Note that the form of the expression (34) differs from (33). This is because in (33) we assume that the decay probability P_{decay}^Y has been previously computed numerically. The latter includes $n_{\bar{Y}}$, which is tightly related to n_Y .

Particle	ϵ_{ann}	$\epsilon_{\mathcal{N}}$
μ^\pm	$3.4 \cdot 10^{-4}$	$\gg 1$
π^\pm	$4.1 \cdot 10^{-2}$	1.15
K^-	$1.4 \cdot 10^{-2}$	$3.4 \cdot 10^{-2}$
K^+	$1.4 \cdot 10^{-2}$	$\gg 1$
K_L	$8.6 \cdot 10^{-4}$	$6.8 \cdot 10^{-2}$
K_S	$2.8 \cdot 10^2$	40.

TABLE II. Ratios (37), (38) for $T = 3$ MeV, $\tau_X = 0.05$ s, and the LLP number density given by eq. (39). The cross-sections are taken from Sec. II. We assumed for simplicity $n_p(T) \approx n_B/2 \approx \eta_B(T) \cdot n_\gamma/2$, with $\eta_B(T \gg m_e) \approx 1.7 \cdot 10^{-9}$.

where we have defined an effective interaction rate with nucleons as

$$\Gamma_{\mathcal{N}} \equiv \sum_{\mathcal{N}} n_{\mathcal{N}} \langle \sigma_{\mathcal{N}}^Y v \rangle \quad (35)$$

Now, let us analyze this solution by considering two limiting cases: $n_Y \langle \sigma_{\text{ann}}^Y v \rangle \gg \Gamma_{\mathcal{N}}$, meaning that annihilations dominate over the interactions with nucleons, and $n_Y \langle \sigma_{\text{ann}}^Y v \rangle \ll \Gamma_{\mathcal{N}}$, which is the opposite.

For the first case, we can estimate the relative importance of decays and annihilations by considering

$$n_Y = \frac{1}{2 \langle \sigma_{\text{ann}}^Y v \rangle \tau_Y} \left[\sqrt{\frac{4}{\epsilon_{\text{ann}}} + 1} - 1 \right], \quad (36)$$

where we have used eq. (34) in the limit $\Gamma_{\mathcal{N}} = 0$ and defined⁷

$$\epsilon_{\text{ann}} = \frac{\tau_Y^{-2}}{n_X \langle \sigma_{\text{ann}}^Y v \rangle} \quad (37)$$

For the second case ($n_Y \langle \sigma_{\text{ann}}^Y v \rangle \ll \Gamma_{\mathcal{N}}$), we can directly compare the decay rate to the rate of the interaction with nucleons, which are both independent of the abundance n_Y :

$$\epsilon_{\mathcal{N}} = \frac{\tau_Y^{-1}}{\Gamma_{\mathcal{N}}} \quad (38)$$

Hence, in both cases, a small value for the ratios (37) and (38) implies that Y decays are much less efficient than the competing processes (annihilations or interactions with nucleons, respectively).

Let us consider the reference choice

$$n_{X,0} = 0.1 \cdot n_{\text{UR}}(T_0) = 0.1 \cdot \frac{\zeta(3)}{\pi^2} T_0^3, \quad (39)$$

⁷ ϵ_{ann} may be understood in the following way. Consider an instant injection of Y from n_X during time $\sim \tau_Y$; during this period, decays do not deplete the Y population. Then, let us assume a priori that the annihilation does not prevent accumulating \bar{Y} during this time, so $n_{\bar{Y}} \approx \frac{n_X}{\tau_X} \tau_Y$. For the ratio of Γ_{decay} and $\Gamma_{\text{ann}} = n_{\bar{Y}} \langle \sigma v \rangle_{\text{ann}}$, one then gets eq. (37).

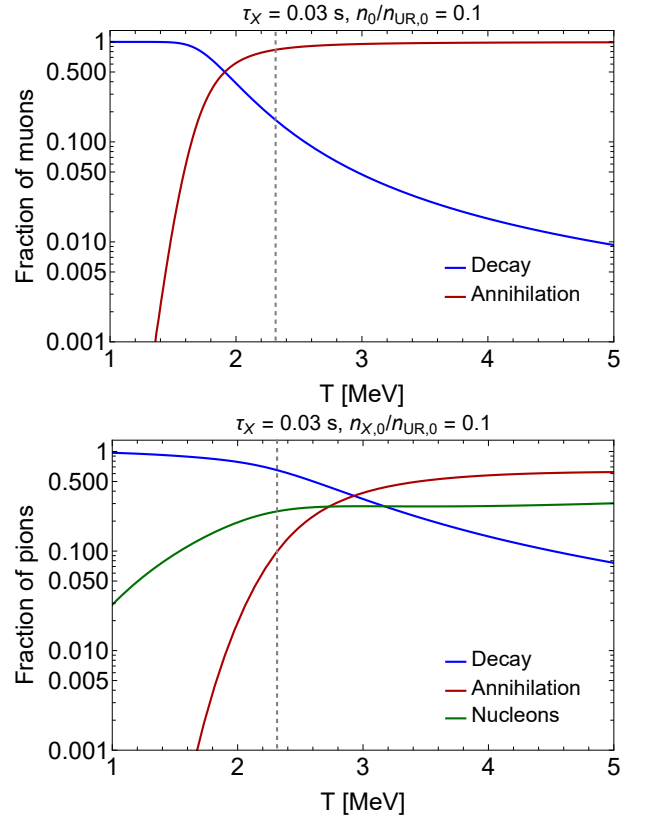


FIG. 2. The yields of muons (top) and pions (bottom) that would decay, annihilate, or interact with the nucleons (Eqs. (30)-(32)) if injected by a decaying particle X with the number density given by eq. (21) and the lifetime $\tau_X = 0.03$ s. The results are obtained using the simplified consideration presented in Sec. IV, in order to be easily reproducible. The vertical dashed line shows the moment of time at which the comoving density of X becomes 0.01 of the $n_{X,0}$, such that the dynamics of X and its decay products already do not affect the Universe.

where n_{UR} is the number density of the ultrarelativistic particle in equilibrium at the given temperature, and $\tau_X = 0.03$ s. The values of the quantities (37) and (38) are shown in Table II. They clearly imply that the dynamics of stopped pions, K^\pm , muons, and K_L may be driven not by decays but by annihilations or interactions with nucleons. For example, the smallness of ϵ_{ann} suggests that the particle prefers to annihilate rather than decay. The exceptions are short-lived K_S : their tiny lifetime allows them to decay before interacting.

The impact of the scattering processes significantly depends on the number density of the interacting counterparts – \bar{Y} for annihilation and baryons for the nucleon interactions. Both $n_{\bar{Y}}$ and n_B are suppressed at low temperatures as $a^{-3} \sim T^3$. In addition, the \bar{Y} number density, entering the annihilation rate for Y s, gets exponentially suppressed at times $t \gg \tau_X$, so the drop in P_{ann}^Y would be much faster than in $P_{\mathcal{N}}^Y$. To account for these effects, we will use the solution (34) and obtain the proba-

bilities (30)-(32) for muons and pions. They are shown in Fig. 2 for the setup (39). For the particular parameters, decays are strongly suppressed at high temperatures but become dominant at a temperature determined by the properties of X . A higher X number density is associated with a lowering of this temperature.

V. QUALITATIVE IMPACT OF THE DYNAMICS OF THE METASTABLE PARTICLES

Let us now qualitatively analyze the impact of the evolution of Y particles on the dynamics of the MeV plasma. We will consider several aspects: properties of primordial neutrinos – N_{eff} , neutrino spectral distortions, the asymmetry in the energy distribution between neutrinos and antineutrinos, and the neutron-to-proton conversion, which sets the initial condition for BBN.

A. N_{eff} and Neutrino Spectral Distortions

The effective number of relativistic neutrino species, N_{eff} , is defined as

$$N_{\text{eff}} = \frac{8}{7} \left(\frac{11}{4} \right)^{\frac{4}{3}} \frac{\rho_{\text{UR}} - \rho_{\gamma}}{\rho_{\gamma}} \Big|_{m_{\nu} \ll T \ll m_e}, \quad (40)$$

where ρ_{UR} and ρ_{γ} represent the energy densities of ultra-relativistic particles and photons, respectively. Under the assumption that neutrinos follow an equilibrium (Fermi-Dirac) distribution, N_{eff} effectively characterizes the neutrino population. However, deviations from thermal equilibrium can lead to a non-thermal neutrino distribution function, $f_{\nu}(p, t)$ and break this degeneracy.

In the Λ CDM framework, the value of N_{eff} is $N_{\text{eff}}^{\Lambda\text{CDM}} \approx 3.04$ [41, 44–50], and the neutrino distribution closely resembles a Fermi-Dirac distribution with temperature $T_{\nu} \approx (4/11)^{1/3} T_{\gamma}$. Variations in N_{eff} and $f_{\nu}(p, t)$ influence the Universe's expansion rate and the neutron-to-proton conversion rates. Specifically, energetic neutrinos can efficiently convert protons to neutrons, thereby increasing the neutron-to-proton ratio beyond the Λ CDM prediction and enhancing primordial helium abundance. Additionally, distortions break the degeneracy between the neutrino energy and number densities, which may be important in the epoch when they become non-relativistic.

Without decays into metastable particles, there are two distinct scenarios:

1. *LLPs decaying solely into EM particles:* In this scenario, the evolution of the neutrino population may be approximately described in terms of the evolution of its temperature [25] (see a discussion in [42]). The resulting deviation in the effective number of relativistic degrees of freedom is

$\Delta N_{\text{eff}} = N_{\text{eff}} - N_{\text{eff}}^{\Lambda\text{CDM}} < 0$, with the neutrino temperature T_{ν} being lower than in the standard case, $T_{\nu} < T_{\nu}^{\Lambda\text{CDM}}$ due to the heating of the EM plasma by the energy injection from the X decays.

2. *LLPs decaying solely into neutrinos:* Decays into neutrinos with thermal energies $E_{\nu} \simeq 3T$ have the opposite effect compared to the pure EM decays: heating the neutrino plasma and increasing N_{eff} . Decays into high-energy neutrinos ($E_{\nu} \gg 3T$) in MeV plasma have a qualitatively different impact. As detailed in [18, 26, 27, 42], they reduce N_{eff} , which arises from two main effects:

- Spectral distortions: high-energy neutrinos interact with thermal neutrinos, enhancing the high-energy tail and depleting the low-energy part of the spectrum. It is important since the rates of the neutrino-EM interaction grow with the energy of the particles.
- Instant thermalization of the EM plasma: any energy injection to the EM sector instantly thermalizes. Without distortions in the spectrum of e^{\pm} particles, the net energy flow is shifted to the EM sector even when the ratio of the energy densities $\rho_{\nu}/\rho_{\text{EM}}$ reaches equilibrium value. As a result, this shift leads to $\Delta N_{\text{eff}} < 0$, analogous to pure EM plasma heating.

As the LLP lifetime τ_X increases, high-energy neutrinos interact less with the EM plasma, reducing the energy transfer and mitigating the negative impact on N_{eff} . For sufficiently large τ_X , ΔN_{eff} becomes positive.

The scenario of LLPs decaying into metastable particles is even more nuanced. Given that $m_Y \gg 3T$, neutrinos from Y decays are typically energetic and resemble the second scenario. However, at MeV temperatures, the decay probability P_{decay}^Y is a lot smaller than unity, meaning that Y particles are more likely to annihilate or interact with nucleons before decaying, effectively suppressing neutrino injection. This behavior mimics pure EM heating. At lower temperatures, as $P_{\text{decay}}^Y \rightarrow 1$, the situation transitions towards the mix between scenarios 1 and 2.

To quantify the impact of the varying P_{decay}^Y on N_{eff} , we define the ratio

$$r_{\nu} = \frac{\rho_{\text{inj},\nu}}{\rho_{\text{inj}}} \Big|_{t=\infty}, \quad (41)$$

which represents the fraction of the LLP's total injected energy ρ_{inj} allocated to neutrinos. ρ_{inj} and the energy density injected into neutrinos $\rho_{\text{inj},\nu}$ evolve according to

$$\frac{d\rho_I}{dt} + 4H\rho_I = \left(\frac{d\rho_I}{dt} \right)_{\text{source}}, \quad (42)$$

where

$$\left(\frac{d\rho_I}{dt}\right)_{\text{source}} = \frac{m_X n_X}{\tau_X} \times \begin{cases} 1, & \rho_I = \rho_{\text{inj}} \\ \xi_{X \rightarrow \nu} + \sum_{y=Y, \bar{Y}} \frac{n_y}{n_X} P_{\text{decay}}^y \xi_{y \rightarrow \nu}, & \rho_I = \rho_{\text{inj}, \nu} \end{cases} \quad (43)$$

Here, $\xi_{A \rightarrow \nu}$ denotes the fraction of the A 's energy injected into the neutrino sector per decay:

$$\xi_{A \rightarrow \nu} = \frac{1}{m_X} \sum_j \text{Br}_{A,j} \langle E_\nu^{(j)} \rangle, \quad (44)$$

with $\text{Br}_{A,j}$ denoting the branching ratio of the j th decay mode of the particle A , and $\langle E_\nu^{(j)} \rangle$ mean energy of neutrinos injected in this decay. When calculating it, we assume that all metastable particles do not decay. As an example, for the decay channel $K^+ \rightarrow \mu^+ + \nu_\mu$, only the neutrino energy is accounted for, whereas the muon is dropped.

The minimum value of r_ν occurs when $P_{\text{decay}}^Y = 0$, implying that only direct X 's decays into neutrinos would contribute. Conversely, the maximum value is achieved when $P_{\text{decay}}^Y = 1$, meaning that all mesons and muons decay:

$$r_{\nu,0} = \frac{1}{m_X} \sum_j \text{Br}_j \cdot \overline{\langle E_\nu^{(j)} \rangle}, \quad (45)$$

where, unlike eq. (44), we include the contribution from inevitable decays when calculating the mean neutrino energy, $\overline{\langle E_\nu^{(j)} \rangle}$. As a cross-check, the expression (43) (and hence r_ν) should give exactly the same results as eq. (45) in the case $P_{\text{decay}}^Y = 1$. We confirm this in Figs. 3, 5, 7 in the limit of large X lifetimes.

When neutrinos from the decay of Y particles effectively decouple, the sign of $\Delta N_{\text{eff}} = N_{\text{eff}} - N_{\text{eff}}^{\Lambda\text{CDM}}$ is determined by whether $r_{\nu,0}$ exceeds the ratio of neutrino to total energy densities in standard cosmology, which for temperatures $T \gtrsim m_e$ is

$$q_\nu = \frac{\rho_\nu}{\rho_\nu + \rho_{\text{EM}}} = \frac{21}{43}. \quad (46)$$

If $r_{\nu,0} > q_\nu$, then ΔN_{eff} increases as τ_X becomes large ($\tau_X \gtrsim 1$ s). Consequently, ΔN_{eff} transitions from negative to positive values as r_ν approaches $r_{\nu,0}$.⁸

B. Neutrino-antineutrino energy asymmetry

Generically, the evolution (22), (29) is not $Y - \bar{Y}$ symmetric due to the term describing the interactions with

nucleons. The reason is that there are no anti-nucleons, which means that the generic interaction rate of Y and \bar{Y} does not have charge conjugation symmetry. This implies that, in general, $n_Y \neq n_{\bar{Y}}$, i.e., metastable particles and antiparticles evolve differently. This asymmetry translates to an asymmetry between neutrinos and antineutrinos via their decays. Let us discuss its qualitative aspects.

The asymmetry may be in number ($n_\nu \neq n_{\bar{\nu}}$) and energy distributions (meaning in particular that $\rho_\nu \neq \rho_{\bar{\nu}}$). In the first case, the net lepton charge $L_\nu \propto n_\nu - n_{\bar{\nu}}$ is generated in the neutrino sector, and the opposite charge $L_l = -L_\nu$ in the electron-positron sector. No sizeable L_ν is induced because we assume that the initial X particle is electrically neutral and the baryon number is conserved. Indeed, the electric charge conservation means that independently of the microscopics of the Y, \bar{Y} evolution, L_l may occur only because of changing the yield of protons. The baryon number conservation implies that this change is bounded by $\eta_B \sim 10^{-9}$. Therefore, we may just assume that $n_\nu = n_{\bar{\nu}}$.

However, the magnitude of the energy asymmetry is not bounded by this argument. First, even if conserving the number of neutrinos, decays of different Y s inject neutrinos with different energies. Namely, decays of kaons release neutrinos with energies as large as $E_{\nu, \text{max}} \approx m_K/2$, decays of pions result in the neutrinos with energy $E_{\nu, \text{max}} \approx 29$ MeV, whereas the maximal neutrino energy from muons decays is $E_{\nu, \text{max}} \approx m_\mu/2$. Second, some Y s, such as kaons, may interact with both protons and neutrons, as well as may or may not convert them, meaning that $\rho_\nu - \rho_{\bar{\nu}}$ may easily exceed the bound $n_B \times E_\nu$ coming from the number asymmetry.

Let us now discuss the energy asymmetry in more detail. If only muons are injected, the nucleon interaction term may be neglected (see a discussion in Sec. II A). If, in addition, the X particle decays into the charged pions, it is important, and we need to analyze it further. Both π^+, π^- interact with nucleons; in addition,

$$\langle \sigma_{\mathcal{N}}^{\pi^\pm} v \rangle = \langle \sigma_{\mathcal{N} \rightarrow \mathcal{N}' v}^{\pi^\pm} \rangle, \quad (47)$$

i.e., pions interact with nucleons solely via converting them (remind eq. (10)). Using this and utilizing the expression for the nucleon abundance X_n from eq. (29), we find that the nucleon interaction terms for π^+, π^- are actually identical:

$$\begin{aligned} n_{\pi^-} \sum_{\mathcal{N}} n_{\mathcal{N}} \langle \sigma_{\mathcal{N}}^{\pi^-} v \rangle &= n_{\pi^+} \sum_{\mathcal{N}} n_{\mathcal{N}} \langle \sigma_{\mathcal{N}}^{\pi^+} v \rangle \\ &= \frac{n_{\pi^-} - n_{\pi^+} \langle \sigma_{p \rightarrow n}^{\pi^-} v \rangle \langle \sigma_{n \rightarrow p}^{\pi^+} v \rangle}{n_{\pi^-} \langle \sigma_{p \rightarrow n}^{\pi^-} v \rangle + n_{\pi^+} \langle \sigma_{n \rightarrow p}^{\pi^+} v \rangle} \end{aligned} \quad (48)$$

The situation is different when charged kaons are injected as well. There is an explicit asymmetry due to the interaction with nucleons: K^+ does not interact with nucleons in the MeV plasma, while K^- participates in various processes with them: interacting with both n and p ,

⁸ Note that q_ν decreases after electron-positron annihilation, allowing for an additional sign change if the LLP decays at $T \lesssim m_e$.

converting $n \leftrightarrow p$ as well as keeping the nucleon type the same (remind Sec. II C). As a result, more K^- would disappear before decaying than K^+ . Decays of K^+ would directly produce muon neutrinos and not antineutrinos. On the other hand, it means that we have more π^+ , μ^+ particles, that decay into antineutrinos.

Overall, this decay asymmetry may induce sizeable differences in the energy distributions of neutrinos and antineutrinos. The energy asymmetry may be split into the ranges $E_\nu > m_\mu/2$, to which only the K decays contribute, and $E_\nu < m_\mu/2$, where the main sources are decays of muons and pions. The first domain is overabundant for neutrinos, whereas the second is for antineutrinos.

A detailed investigation of this question goes beyond the scope of this paper, as it requires the development of efficient methods to solve the neutrino Boltzmann equation in the presence of high-energy neutrinos and neutrino-antineutrino asymmetry. We leave the quantitative study of this intriguing question using the approach from [26, 27] for future work.

C. Evolution of the n/p ratio

As was mentioned in Sec. III, injecting mesons into the primordial plasma significantly modifies the dynamics of the n/p ratio n_n/n_p . Overall, the effect of the meson-driven $p \leftrightarrow n$ conversion is well-known [4, 8, 36, 37], but let us describe it shortly. In Λ CDM, the n/p ratio is suppressed by the Boltzmann exponent as far as weak interactions maintain chemical equilibrium between the neutrons and protons:

$$\frac{n_n}{n_p} \approx \exp\left[-\frac{m_n - m_p}{T}\right] \quad (49)$$

Once mesons are injected, they increase the ratio above the value (49). This is mainly because meson-driven $p \leftrightarrow n$ conversion is thresholdless. The BBN constraint on LLP lifetimes may be imposed from the requirement on this enlarged ratio to relax to the Λ CDM value within the margin determined by the error in the primordial helium measurements [8]. The meson-driven $p \leftrightarrow n$ conversion cross-section is orders of magnitude higher than the one for the weak conversion, and even exponentially suppressed amounts of mesons (at times $t \gg \tau_X$) completely drive the dynamics of the n/p ratio. Because of this, the resulting constraint on the LLP's lifetime depends on the LLP's initial number density and the yield of mesons available for the conversion only logarithmically [8, eq. (11)].

Because of the same reason, the meson-driven $p \leftrightarrow n$ conversion typically dominates over other effects of LLPs on the dynamics of the n/p ratio, including the modified expansion of the Universe and neutrino properties. For example, consider Heavy Neutral Leptons with lifetimes $\tau_N \simeq 0.02$ s and heavy enough to decay into mesons.

While barely modifying N_{eff} , they induce a huge change in the n/p ratio due to mesons [8, 17].

The only modification of this picture due to our study comes from adding the meson annihilation processes. They suppress the yield of mesons available for the $p \leftrightarrow n$ conversion, eq. (32). However, the suppression is maximum a factor of few (remind Fig. 2), which would modify the BBN constraint in a minor way as it enters the logarithm.

VI. CASE STUDIES

In this section, we consider the impact of the evolution of Y_s on neutrinos for three models: A toy model adding a particle with constant abundance decaying into charged pions, Higgs-like scalars, and Heavy Neutral Leptons (HNLs). We will discuss the mass and lifetime dependence of the overall energy fraction injected into neutrinos, eq. (41), and the effect on the neutrino distributions. We compute the neutrino distribution using the approach of Ref. [42]. It utilizes solving the neutrino Boltzmann equation in the presence of the LLPs using the comoving momentum discretization approach firstly developed in [51] and further implemented in [41].

A. Toy model: LLPs decaying into pions

Consider a toy model with the LLP X decaying solely into charged pions:

$$N_{\pi^\pm}^X = 1, \quad N_{\mu,K}^X = 0 \quad (50)$$

It means that no kaons are involved, but there still would be muons originating from the pion decay, remind eq. (7). To make the analysis as transparent as possible, the X 's abundance is chosen to be a constant:

$$\mathcal{Y}_{\text{LLP}} \equiv \left(\frac{n_{\text{LLP}}}{s}\right)_{T=10 \text{ MeV}} = 2 \cdot 10^{-3} \quad (51)$$

It corresponds to the scenario in which the particle X was in thermal equilibrium and decoupled while still being relativistic.

We focus on masses above the threshold $m_X > 2m_\pi \approx 0.28$ GeV. Regarding the lifetimes, following the discussion in Sec. V, we test the range $0.01 \text{ s} < \tau_X < 10 \text{ s}$. Let us first discuss how X would distribute its energy among the neutrino and the EM sectors. Upon decay, it will produce a pair of pions whose non-trivial evolution has been discussed before. Injection into the neutrino sector would occur only in the case of decay of a charged pion which would produce a muon and a muon antineutrino; the resulting muon may then decay into an electron, an electron antineutrino, and a muon neutrino. In total, roughly $r_{\nu,0}^\pi \approx 70\%$ of the pion mass would go to the neutrino sector if the pion and the subsequently produced muon inevitably decay. In this case, the injection

into the EM sector will be composed of the initial kinetic energy of the pion $(m_X - 2 \cdot m_\pi)/2$ and the EM part of the muon decay, which will be approximately 30% of its mass. This gives us the maximal possible fraction of the energy of the X particle directly injected in the neutrino sector:

$$r_{\nu,0} \approx \frac{2m_\pi \cdot r_{\nu,0}^\pi}{m_X} \approx q_\nu \cdot \frac{388 \text{ MeV}}{m_X}, \quad (52)$$

where q_ν is the Λ CDM ratio (46). Provided that there are no interactions of neutrinos with the EM plasma, if $r_{\nu,0}$ exceeds this ratio (i.e., $m_X < 388 \text{ MeV}$), the correction ΔN_{eff} would be positive in the limit of large lifetimes (remind the discussion in the previous section).

The disappearance of the pions and muons because of annihilation and interaction with nucleons spoils this picture. We illustrate this by calculating the quantity $r_\nu(m_X, \tau_X)$, see Fig. 3. At small lifetimes $\tau_X \lesssim 0.5 \text{ s}$, pions and muons produced in X decays would prefer to disappear before decaying. This leads to a significant drop $r_\nu \ll r_{\nu,0}$. With the increase of the lifetime, more and more Y s would decay, and r_ν tends to the maximal possible value $r_{\nu,0}$.

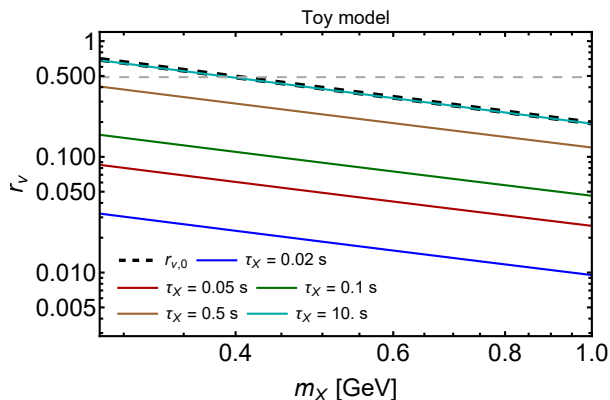


FIG. 3. The evolution of the fraction injected into neutrinos r_ν , eq. (41), for the model of a hypothetical particle X with the abundance given by eq. (51) and decaying solely into a pair of the charged pions. The grey dashed line shows the value $r_\nu = 21/43$, for which $\Delta N_{\text{eff}} = 0$ in the absence of the neutrino-EM interactions (see a discussion around eq. (46)). Different solid lines show the behavior of r_ν for the lifetimes ranging from 0.02 to 10 s. The generic pattern is that for the fixed mass $r_\nu(\tau_X)$ is smallest at small lifetimes $\tau_X \ll 1 \text{ s}$, which is due to the high chance of the disappearance of pions and muons due to annihilation and interactions with nucleons. Once lifetime increases, it grows and approaches the value $r_{\nu,0}$ (the dashed black line), which is when all pions and muons inevitably decay (eq. (52)). The pattern occurs since scattering and annihilation processes become less efficient at lower temperatures. The slope of the lines represents the increasing kinetic energy of the pion as a function of the LLP mass; it gets immediately transferred to the EM sector.

Now, let us discuss the impact on N_{eff} for this toy model. The plot with ΔN_{eff} as a function of X mass

and lifetime is shown in the upper panel of Fig. 4. Two representative choices for the mass of X are considered: $m_X = 282 \text{ MeV}$, for which $r_{\nu,0} > q_\nu$ (and hence ΔN_{eff} would be positive at large lifetimes), and $m_X = 550 \text{ MeV}$, for which $r_{\nu,0} < q_\nu$. To highlight the impact of the Y evolution on the properties of neutrinos, we show the results for two setups – the one assuming $P_{\text{decay}}^Y = 1$ (i.e., when the decays are inevitable), and the one including the full evolution of Y s, i.e. accounting for annihilations and interactions with nucleons (which we will call below the realistic setup).

The behavior of the curves in Fig. 4 is in agreement with the qualitative discussion in Sec. V and in this section. For the lifetimes $\tau_X \ll 10 \text{ s}$ and both masses, there are severe differences in ΔN_{eff} between the two setups. The realistic setup corresponds to a lower ΔN_{eff} ; this is expected since the decay of Y particles injects more energy directly into the EM sector. In the limit of large lifetimes $\tau_X \rightarrow 10 \text{ s}$, the two results match, as annihilation and interactions with nucleons become irrelevant.

To investigate the impact of the Y disappearance further, let us consider the ratio of the mean neutrino energies after the electron-positron annihilation for these two setups, see the lower panel of Fig. 4. The setup with $P_{\text{decay}}^Y = 1$ leads to higher neutrino energies, which is expected, as we have a more abundant high-energy neutrino tail.

B. Higgs-like scalars

Let us now consider a particular model of long-lived particles. We start with Higgs-like scalars S [28]. We will concentrate on the minimal model, with the effective Lagrangian

$$\mathcal{L} = \theta m_h^2 h S + \mathcal{L}_{\text{kinetic}} \quad (53)$$

Here, h is the Higgs boson, and θ is the mixing angle, with $|\theta| \ll 1$. Due to the mass mixing, the scalars have a similar interaction pattern as h (so Yukawa couplings to the SM fermions), with the couplings additionally suppressed by θ .

The main decay modes of these scalars in the GeV mass range are two-body decays into particle-antiparticle pairs:

$$S \rightarrow e^+e^-/\mu^+\mu^-/\pi^+\pi^-/2\pi^0/K^+K^-/K_LK_S, \quad (54)$$

with the decays into heavier particles dominating once they become kinematically possible. The fraction of energy injected into neutrinos $r_{\nu,0}$ by the scalar decays is shown in Fig. 5. It is exactly zero for masses $m_S < 2m_\mu$, because the only available scalar decay modes are into the EM particles. Then, it gets rapidly enhanced at $m_S = 2m_\mu$ and $m_S = 2m_K$ – the mass thresholds where decays into two muons and kaons open up. In the domain of intermediate masses, it gradually decreases as the decay products have more and more kinetic energy that gets stored in the EM plasma.

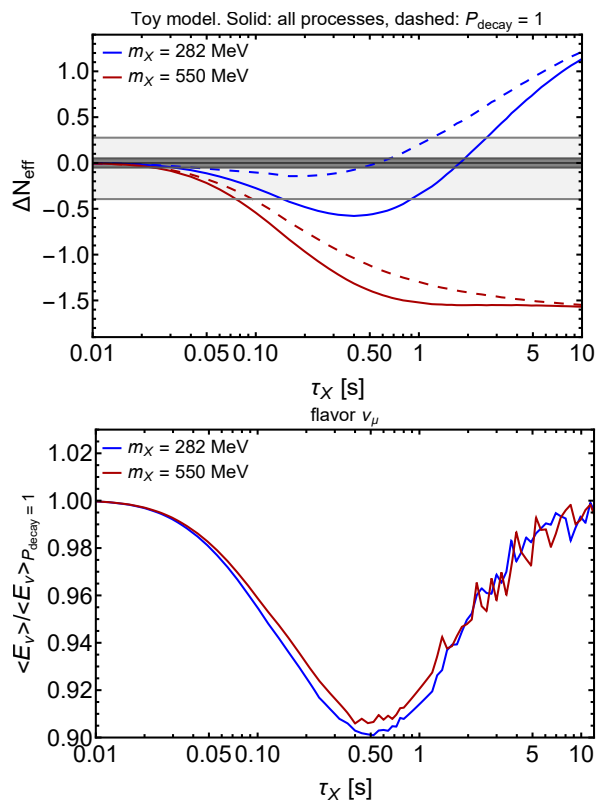


FIG. 4. The effect of the evolution of Y_s on the properties of neutrinos for the same LLP model as in Fig. 3. Two LLP masses are considered – $m_X = 282$ MeV and 550 MeV, representing the cases when ΔN_{eff} tends, correspondingly, to a positive and negative value in the limit of large lifetimes (see a discussion in Sec. VIA). The results are obtained using the unintegrated neutrino Boltzmann equation solver from [42]. To highlight the importance of the annihilation and interactions with nucleons, we consider two setups – the one that includes annihilation and interactions with nucleons (the realistic setup) and the one that includes solely decays and kinetic energy loss, which corresponds to the commonly assumed case $P_{\text{decay}}^Y = 1$. *Top panel:* the correction ΔN_{eff} . The gray band represents the Planck 95% CL constraints $N_{\text{eff}} = 2.99^{+0.33}_{-0.34}$ [43], whereas the black band shows the forecast of the accuracy of the measurements performed by the Simons Observatory, which we assume to be centered at $\Delta N_{\text{eff}} = 0$ [52]. *Bottom panel:* the ratio of the mean energies of the muon neutrinos in the realistic setup case to the setup $P_{\text{decay}} = 1$, as a function of the X 's lifetime. The numerical noise in the domain of large lifetimes is caused by the precision limit of the Boltzmann solver.

The cosmological production and constraints of S have been studied in [14, 15]. Among the cosmological effects of the scalars, it studied the impact of the Higgs-like scalars on neutrinos. The analysis was simplified by considering a version of the integrated neutrino Boltzmann equation and also assuming that $Y = \mu, \pi, K$ decay after thermalizing their kinetic energy. Under this approximation, ΔN_{eff} is determined by whether $r_{\nu,0}$ exceeds the quantity q_ν during decays of the scalar. This is the case

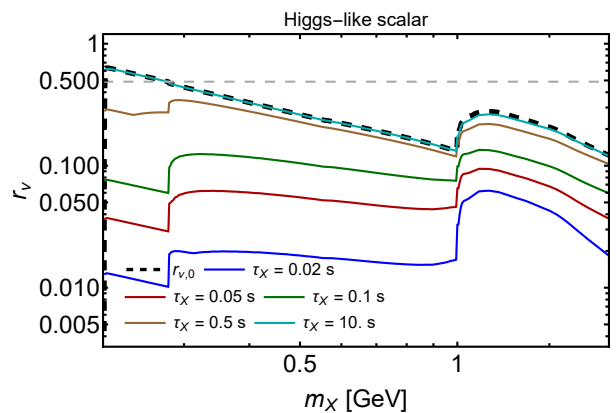


FIG. 5. The fraction of energy injected into neutrinos in decays of Higgs-like scalar decays, see eq. (41). The solid lines correspond to different scalar lifetimes, whereas the dashed black line is obtained under the usual assumption that all the metastable particles decay. The rapid change at the masses $m_X = 2m_\mu, 2m_\pi, 2m_K$ is caused by the opening of the decay into the pair of corresponding particles. The horizontal gray dashed line denotes the value of $r_{\nu,0}$ for which the injections would increase the neutrino-to-EM energy density ratio if assuming no interactions in the primordial plasma (see a discussion around eq. (46)).

in the region $2m_\mu < m_S \lesssim 2m_\pi$.

Let us now include the effects of mesons and muons evolution as well as momentum-dependent (unintegrated) Boltzmann equations for the neutrino distributions. In Fig. 5, we show the mass-lifetime dependence of r_ν including the impact of annihilation and interactions. Similarly to the case of the toy model decaying into pions, the generic pattern is that $r_\nu(\tau_S) \rightarrow 0$ for small scalar lifetimes and reaches $r_{\nu,0}$ for the lifetimes $\simeq 10$ s. In particular, the ratio r_ν becomes less than 5% (and so most of the scalar's energy goes to the EM sector) for the lifetimes $\tau_S \lesssim 0.05$ s. r_ν jumps at $m_S = 2m_\pi$, which is caused by the opening of the di-pion decay channel. The pions (the main decay products in the mass range $2m_\pi < m_S < 2m_K$) have a larger decay probability than the muons, which means that they have a higher chance to release energy into neutrinos than muons. The behavior of ΔN_{eff} is shown in Fig. 6. In the mass range $2m_\mu < m_S \lesssim 2m_\pi$, increasing the scalar lifetime, we see the transition between negative and positive changes in N_{eff} . It is caused by tending $r_\nu \rightarrow r_{\nu,0} > q_\nu$. At higher masses, $r_{\nu,0} < q_\nu$, so in any case, ΔN_{eff} remains negative.

C. Heavy Neutral Leptons

Let us now consider Heavy Neutral Leptons. The Lagrangian of HNLs has the form

$$\mathcal{L} = y_\alpha \bar{L}_\alpha \tilde{H} \text{HNL} + \text{h.c.}, \quad (55)$$

where α denotes the SM lepton generation, L_α is the corresponding left doublet, y_α is the Yukawa interaction

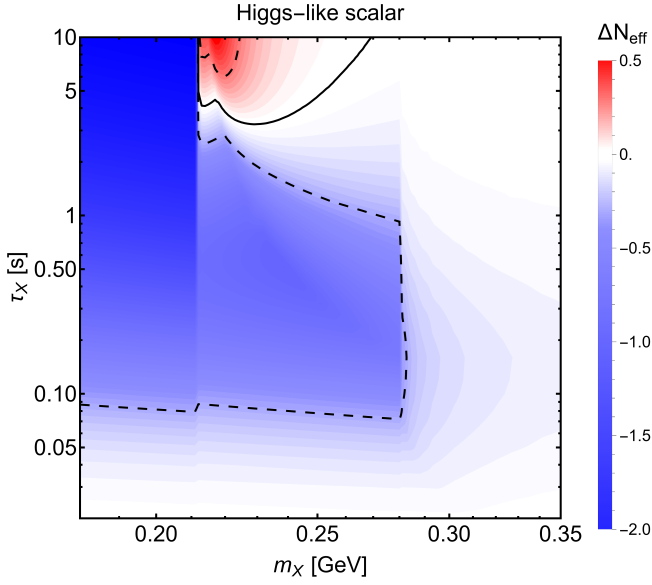


FIG. 6. The effect of the presence of the Higgs-like scalars on the correction $\Delta N_{\text{eff}} = N_{\text{eff}} - N_{\text{eff}}^{\Lambda\text{CDM}}$. The solid black line shows the parameter space where $\Delta N_{\text{eff}} = 0$, whereas the dashed black lines denote the domain where ΔN_{eff} are beyond the lower and upper bounds of the N_{eff} measurements as extracted from Planck measurements [53]. The change in the sign of ΔN_{eff} is driven by the dynamics of metastable particles produced by S 's decays. The decrease of the magnitude of $|\Delta N_{\text{eff}}|$ with the scalar mass is caused by the scaling of the scalar abundance $\mathcal{Y}_S(m_S) \propto \Gamma_S^{-1}(m_S, \theta = 1)$, where Γ_S is the scalar decay width (see [14] and [42] for details).

coupling, while $\tilde{H} = i\sigma_2 H^*$ is the Higgs doublet in the conjugated representation. Effectively, HNLs interact as heavy neutrinos, with the interaction coupling being suppressed by the mixing angle $U_\alpha \simeq y_\alpha v_H / m_{\text{HNL}}$, where v_H is the Higgs VEV [35]. We will consider the case of HNLs mixing with the muon neutrinos ν_μ , keeping in mind that the other cases are similar.

Let us briefly discuss the production of HNLs. In high-temperature plasma, the mixing angle gets modified because of the thermal neutrino self-energy correction. In particular, in the plasma without the lepton asymmetry at temperatures $T \gtrsim 1$ GeV, the effective mixing angle is given by

$$U_m^2(T) \approx \frac{U^2}{\left[1 + 9.6 \cdot 10^{-24} \left(\frac{T}{1 \text{ MeV}}\right)^6 \left(\frac{m_{\text{HNL}}}{150 \text{ MeV}}\right)^{-2}\right]^2}, \quad (56)$$

where m_{HNL} is the HNL mass. The scaling of the HNL production rate with temperature is $\Gamma_{\text{int}} \sim G_F^2 T^5 U_m^2$, with G_F being the Fermi coupling. Comparing the HNL interaction rate with the Hubble rate H , we may establish whether HNLs entered the thermal equilibrium. Namely, the ratio Γ_{int}/H is $\ll 1$ at high temperatures T because of the suppression of $U_m(T)$, then reaches the peak value at $T_{\text{peak}} \approx 12 \text{ GeV} (m_{\text{HNL}}/(1 \text{ GeV}))^{1/3}$ GeV, and then starts decreasing, since Γ_{int} drops with T faster than H .

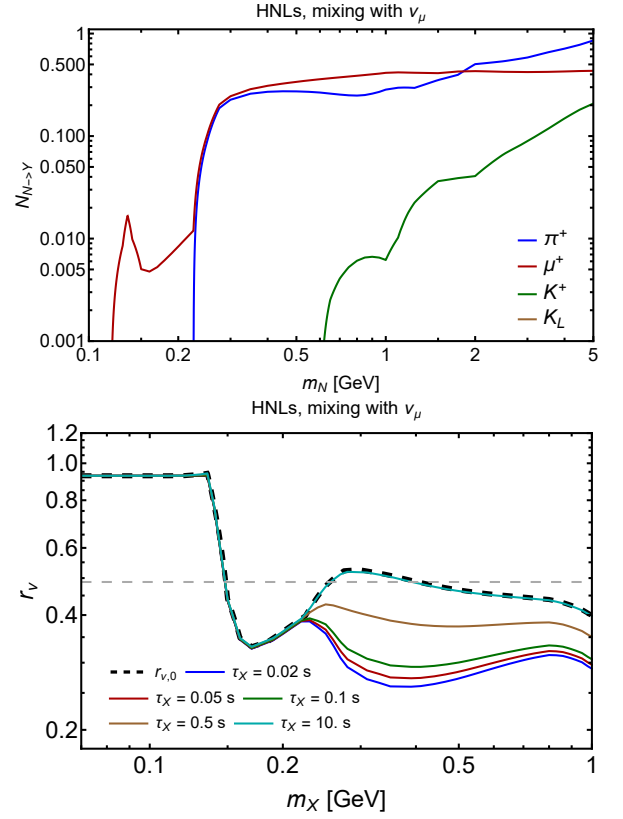


FIG. 7. How HNLs affect the neutrino population. Top panel: the fractions of the metastable particles $Y = \mu^\pm, \pi^\pm, K^\pm$ per HNL decay. Bottom panel: the dependence of r_ν on the HNL lifetime. The minimal value of r_ν corresponds to the situation when all mesons and muons disappear without decaying; then, r_ν is saturated solely by direct decays into neutrinos.

If the rate-to-Hubble ratio at T_{peak} is < 1 , HNLs never entered thermal equilibrium.

We have calculated the HNL abundance following the approach similar to the one used in Ref. [8]. To compute the kinematics of HNL decay products, we used the **SensCalc** package [54], which we have modified to account for transferring of all the kinetic energy of the charged metastable particles to the EM plasma and forbid the mesons and muons to decay. We used the exclusive decays below the HNL mass $m_{\text{HNL}} \simeq 1$ GeV and decays into jets above this mass, with showering and hadronization performed using **PYTHIA8** [55]. The amounts of the charged pions, muons, and kaons per HNL mass are shown in Fig. 7 (top panel).

Using the machinery we described above, we computed the quantity r_ν , see the same figure (bottom panel). Unlike the models we considered above, the decay palette of the HNLs includes processes directly injecting neutrinos. They are

$$\text{HNL} \rightarrow \nu_\alpha \bar{\nu}_\alpha \nu_\beta, \quad \text{HNL} \rightarrow \text{hadrons} + \nu_\beta, \quad (57)$$

where “hadrons” denote either a single meson such as π^0 or a multi-meson state, depending on the HNL mass [35].

Therefore, even if all the mesons and muons disappear without decaying, the quantity r_ν would be non-zero even for short HNL lifetimes $\tau_{\text{HNL}} \lesssim 0.1$ s. However, the fraction to be injected by meson decays is still large, depending on the HNL mass.

Because of the presence of the direct decays into neutrinos, computing the impact of HNLs on the primordial neutrinos is much more complicated: the traditional approaches of solving the neutrino Boltzmann equation based on the discretization of the comoving momentum space would take a too large amount of time to evolve the neutrino distribution function. We will return to this in future work. Nevertheless, Fig. 7 shows the importance of careful tracing of the evolution of the metastable particles in the HNL case.

VII. CONCLUSIONS

Many new physics scenarios introduce long-lived heavy particles X , that decay into metastable Standard Model (SM) particles Y , such as muons, pions, and kaons. Examples of such X particles include Higgs-like scalars, dark photons, axion-like particles, and others. The lifetimes of the Y particles are sufficiently long to allow numerous interactions with components of the primordial plasma, including electromagnetic particles and nucleons. These interactions significantly modify the evolution of Y abundances and, consequently, affect the properties of primordial neutrinos.

In this work, we conducted a detailed study of Y particle evolution, incorporating processes such as annihilation with antiparticles, interactions with nucleons, elastic electromagnetic scattering, and decays (see Sec. II). Notably, annihilation processes are examined here for the first time, while interactions with nucleons have previously been considered only regarding Big Bang Nucleosynthesis (BBN) and not when studying the impact on neutrinos.

In order to analyze the coupled dynamics of Y particles and nucleon densities, we have developed a systematic approach based on the system of the integrated Boltzmann equations on their number densities (Sec. III). Applying its simplified version to muons and pions, we have demonstrated that at MeV temperatures, Y particles predominantly annihilate or interact with nucleons rather than decay (Sec. IV).

Incorporating these effects substantially alters the influence of new physics on neutrino properties (Sec. V). Specifically, when Y particles decay, a significant fraction of their mass energy is transferred to the neutrino sector, inducing spectral distortions. Conversely, if Y particles disappear without decaying, their energy is instead fully transferred to the electromagnetic sector. Additionally, the differential decay rates of kaons and antikaons lead to asymmetries in the energy distributions of neutrinos and antineutrinos, which may persist if injections occur during neutrino decoupling (Sec. VB). A comprehensive

analysis of this intriguing question is left for future work.

We applied our methodology to specific models, including a toy model with pions (Sec. VIA), Higgs-like scalars (Sec. VIB), and Heavy Neutral Leptons (HNLs, Sec. VIC). Our findings reveal significant deviations from state-of-the-art studies assuming inevitable decays, including changes in both the magnitude and sign of ΔN_{eff} and alterations in the neutrino distribution functions, as illustrated in Figs. 4 and 6. A detailed discussion of the approach we use to solve the neutrino Boltzmann equations in the presence of metastable particles will be provided in the upcoming paper [42].

In summary, our results provide a deeper understanding of how long-lived particles influence the neutrino population in the Early Universe. To facilitate further research, we have made available a public `Mathematica` code that implements our approach.

ACKNOWLEDGEMENTS

This work has received support by the European Union's Framework Programme for Research and Innovation Horizon 2020 under grant H2020-MSCA-ITN-2019/860881-HIDDeN, JSPS Grant-in-Aid for Scientific Research KAKENHI Grant No. 24KJ0060. K.A is grateful to Maksym Ovchynnikov and Thomas Schwetz for the hospitality during the stay at the Institute for Astroparticle Physics, KIT. The authors thank Miguel Escudero for carefully reading the manuscript and for providing useful comments.

Appendix A: Mathematica code

In this Appendix, we discuss the `Mathematica` code that traces the evolution of the metastable particles in the presence of the decaying LLPs X ; it is available on [GitHub/maksymovchynnikov/Metastable-dynamics](https://github.com/maksymovchynnikov/Metastable-dynamics) and [10.5281/zenodo.14020343](https://zenodo.org/record/14020343). The Zenodo repository also contains pre-computed data for some LLP models.

The central notebook is `main.nb`. Once launching its initialization cells, it first calls secondary notebooks with all the necessary definitions. The secondary notebooks are located in the folder `codes/Secondary particles evolution`. They are: `parameters-functions.nb`, defining various parameters and analytic functions; `cross-sections.nb`, containing the calculations of various interaction rates involving Y s; `universe-simplified-dynamics.nb`, containing a simplified description of the thermodynamics following the approach of [25]; `evolution-Ys.nb`, which brings all the processes with Y s altogether and defines the system of the Boltzmann equations on the Y s' number densities, depending of various options and properties of the X particles; and `final-system.nb`, which uses these codes to calculate the impact of the decaying LLPs with Y decay products. Apart from that, the folder `SM_Rates` contains useful definitions such as effective Lagrangians, tabulated energy densities of electrons, and oscillation probabilities.

Once all secondary codes are called, users may proceed with applying the main notebook to study various physics cases. As an input for the model, the code requires various properties. The input for the implemented models is stored in the section `LLP input`. Each of its sub-sections is dedicated to a separate model.

For the given model LLP, the main definitions are

- `τ LLP[LLP, mass, coupling]`, which describes the dependence of the lifetime on LLP's mass and coupling;
- `nLLPini[LLP, mN, τ]`, which is the number density of the LLP in the units of GeV^3 at $T = 20 \text{ MeV}$, $n_{X,\text{ini}}$; the code assumes that the LLPs are already decoupled at that epoch.
- `{ $\xi_{\text{to}\nu}$ [LLP, ν_e , mass], $\xi_{\text{to}\nu}$ [LLP, ν_μ , mass], $\xi_{\text{to}\nu}$ [LLP, ν_τ , mass]}`, which are the mass-dependent fractions of the LLP's mass injected *directly* in the neutrino sector, the flavor ν_α .
- `NtoY[LLP, Y, mass]` – the amount of the Y particles produced per LLP's decay.
- `EnergyFractionsTo ν [LLP, "Total", mass]`, which is the total fraction injected into neutrinos, assuming that all Y particles inevitably decay.

The section *Generating the evolution of Y s* is devoted to generating the data for the grid of masses and lifetimes of the given LLPs: `MassGrid[LLP]`, `lifetimeGrid[LLP]`, defined in subsection *Definitions*. Subsection *Launching for mass and lifetime grids* launches the system of equations for the given LLP model, mass and lifetime grids. This is done with the help of the routine `exportBlockFullData[LLP, IfDecayOnlyLLP[LLP]]`, where the parameter `IfDecayOnlyLLP[LLP]` may be `True` (if annihilation and the interactions with nucleons are turned off) or `False` (if they are included). For each mass and lifetime, this routine launches

```
mergedFunction[LLP, mass,  $\tau$ , Ylist, DecayOnly]
```

which returns the following data row:

```
{mass,  $\tau$ ,  $n_{X,\text{ini}}$ ,  $N_{\text{eff}}$ ,  $r_1$ ,  $r_\nu$ ,  $r_3$ ,  $N_{\mu^+}^X$ ,  $N_{\pi^+}^X$ ,  $N_{K^+}^X$ ,  $N_{K_L}^X$ ,  $r_{\nu,0}$ }, tabulated decay probabilities for Ylist}
```

Here, the value of N_{eff} is obtained via the integrated approach of Ref. [25], r_1 is the cumulative fraction of the total energy density injected by LLP to the total energy density of the Universe, r_3 is the ratio of the energy density injected into the neutrino sector to the total neutrino energy density. The quantities N_Y^X are defined around eq. (22), while $r_\nu, r_{\nu,0}$ are given by eqs. (41), (45). The dependence of the tabulated decay probabilities is chosen of the form `{Temperature in MeV, P_{decay}^Y }`.

The routine `exportOutputForCluster[LLP]` prepares the data for the unintegrated Boltzmann solver for the neutrino Boltzmann equation, which will be discussed in [42].

Section *Plots - global numbers* first imports the generated datasets (subsection *Data importing*) and then makes plots (subsection *Plots*). The imported data has the names `OutputLLPintegrated[LLP]` and `OutputLLPUnintegrated[LLPsel]`, correspondingly for the output of the notebook and the solver from [42]. The latter is pre-computed for some models and may be found in the associated Zenodo repository. Each subsection (e.g., r_ν), contains definitions needed to make a plot for each model (say, `{mminPlot[LLP, " r_ν "], mmaxPlot[LLP, " r_ν "]}`) defines the LLP mass range for the r_ν plot), as well as the code making the plot itself.

[1] A. D. Dolgov, "Neutrinos in cosmology," *Phys. Rept.* **370** (2002) 333–535, [arXiv:hep-ph/0202122](https://arxiv.org/abs/hep-ph/0202122).

- [2] S. Sarkar, “Big bang nucleosynthesis and physics beyond the standard model,” *Rept. Prog. Phys.* **59** (1996) 1493–1610, [arXiv:hep-ph/9602260](#).
- [3] A. D. Dolgov, S. H. Hansen, G. Raffelt, and D. V. Semikoz, “Heavy sterile neutrinos: Bounds from big bang nucleosynthesis and SN1987A,” *Nucl. Phys. B* **590** (2000) 562–574, [arXiv:hep-ph/0008138](#).
- [4] K. Kohri, “Primordial nucleosynthesis and hadronic decay of a massive particle with a relatively short lifetime,” *Phys. Rev. D* **64** (2001) 043515, [arXiv:astro-ph/0103411](#).
- [5] S. Hannestad, “What is the lowest possible reheating temperature?,” *Phys. Rev. D* **70** (2004) 043506, [arXiv:astro-ph/0403291](#).
- [6] M. Pospelov and J. Pradler, “Big Bang Nucleosynthesis as a Probe of New Physics,” *Ann. Rev. Nucl. Part. Sci.* **60** (2010) 539–568, [arXiv:1011.1054 \[hep-ph\]](#).
- [7] M. Kawasaki, K. Kohri, T. Moroi, and Y. Takaesu, “Revisiting Big-Bang Nucleosynthesis Constraints on Long-Lived Decaying Particles,” *Phys. Rev. D* **97** (2018) no. 2, 023502, [arXiv:1709.01211 \[hep-ph\]](#).
- [8] A. Boyarsky, M. Ovchinnikov, O. Ruchayskiy, and V. Syvolap, “Improved big bang nucleosynthesis constraints on heavy neutral leptons,” *Phys. Rev. D* **104** (2021) no. 2, 023517, [arXiv:2008.00749 \[hep-ph\]](#).
- [9] J. R. Ellis, J. E. Kim, and D. V. Nanopoulos, “Cosmological Gravitino Regeneration and Decay,” *Phys. Lett. B* **145** (1984) 181–186.
- [10] T. Moroi, H. Murayama, and M. Yamaguchi, “Cosmological constraints on the light stable gravitino,” *Phys. Lett. B* **303** (1993) 289–294.
- [11] M. Kawasaki and T. Moroi, “Gravitino production in the inflationary universe and the effects on big bang nucleosynthesis,” *Prog. Theor. Phys.* **93** (1995) 879–900, [arXiv:hep-ph/9403364](#).
- [12] G. F. Giudice, E. W. Kolb, and A. Riotto, “Largest temperature of the radiation era and its cosmological implications,” *Phys. Rev. D* **64** (2001) 023508, [arXiv:hep-ph/0005123](#).
- [13] T. Kanzaki, M. Kawasaki, K. Kohri, and T. Moroi, “Cosmological Constraints on Neutrino Injection,” *Phys. Rev. D* **76** (2007) 105017, [arXiv:0705.1200 \[hep-ph\]](#).
- [14] A. Fradette and M. Pospelov, “BBN for the LHC: constraints on lifetimes of the Higgs portal scalars,” *Phys. Rev. D* **96** (2017) no. 7, 075033, [arXiv:1706.01920 \[hep-ph\]](#).
- [15] A. Fradette, M. Pospelov, J. Pradler, and A. Ritz, “Cosmological beam dump: constraints on dark scalars mixed with the Higgs boson,” *Phys. Rev. D* **99** (2019) no. 7, 075004, [arXiv:1812.07585 \[hep-ph\]](#).
- [16] T. Hasegawa, N. Hiroshima, K. Kohri, R. S. L. Hansen, T. Tram, and S. Hannestad, “MeV-scale reheating temperature and thermalization of oscillating neutrinos by radiative and hadronic decays of massive particles,” *JCAP* **12** (2019) 012, [arXiv:1908.10189 \[hep-ph\]](#).
- [17] N. Sabti, A. Magalich, and A. Filimonova, “An Extended Analysis of Heavy Neutral Leptons during Big Bang Nucleosynthesis,” *JCAP* **11** (2020) 056, [arXiv:2006.07387 \[hep-ph\]](#).
- [18] A. Boyarsky, M. Ovchinnikov, N. Sabti, and V. Syvolap, “When feebly interacting massive particles decay into neutrinos: The Neff story,” *Phys. Rev. D* **104** (2021) no. 3, 035006, [arXiv:2103.09831 \[hep-ph\]](#).
- [19] L. Mastrototaro, P. D. Serpico, A. Mirizzi, and N. Saviano, “Massive sterile neutrinos in the early Universe: From thermal decoupling to cosmological constraints,” *Phys. Rev. D* **104** (2021) no. 1, 016026, [arXiv:2104.11752 \[hep-ph\]](#).
- [20] H. Rasmussen, A. McNichol, G. M. Fuller, and C. T. Kishimoto, “Effects of an intermediate mass sterile neutrino population on the early Universe,” *Phys. Rev. D* **105** (2022) no. 8, 083513, [arXiv:2109.11176 \[hep-ph\]](#).
- [21] J. Alvey, M. Escudero, and N. Sabti, “What can CMB observations tell us about the neutrino distribution function?,” *JCAP* **02** (2022) no. 02, 037, [arXiv:2111.12726 \[astro-ph.CO\]](#).
- [22] J. Alvey, M. Escudero, N. Sabti, and T. Schwetz, “Cosmic neutrino background detection in large-neutrino-mass cosmologies,” *Phys. Rev. D* **105** (2022) no. 6, 063501, [arXiv:2111.14870 \[hep-ph\]](#).
- [23] M. Escudero, T. Schwetz, and J. Terol-Calvo, “A seesaw model for large neutrino masses in concordance with cosmology,” *JHEP* **02** (2023) 142, [arXiv:2211.01729 \[hep-ph\]](#). [Addendum: *JHEP* 06, 119 (2024)].
- [24] D. Naredo-Tuero, M. Escudero, E. Fernández-Martínez, X. Marciano, and V. Poulin, “Living at the Edge: A Critical Look at the Cosmological Neutrino Mass Bound,” [arXiv:2407.13831 \[astro-ph.CO\]](#).
- [25] M. Escudero Abenza, “Precision early universe thermodynamics made simple: N_{eff} and neutrino decoupling in the Standard Model and beyond,” *JCAP* **05** (2020) 048, [arXiv:2001.04466 \[hep-ph\]](#).
- [26] M. Ovchinnikov and V. Syvolap, “How new physics affects primordial neutrinos decoupling: Direct Simulation Monte Carlo approach,” [arXiv:2409.07378 \[astro-ph.CO\]](#).
- [27] M. Ovchinnikov and V. Syvolap, “Primordial neutrinos and new physics: novel approach to solving neutrino Boltzmann equation,” [arXiv:2409.15129 \[hep-ph\]](#).
- [28] I. Boiarska, K. Bondarenko, A. Boyarsky, V. Gorkavenko, M. Ovchinnikov, and A. Sokolenko, “Phenomenology of GeV-scale scalar portal,” *JHEP* **11** (2019) 162, [arXiv:1904.10447 \[hep-ph\]](#).
- [29] J. Beacham *et al.*, “Physics Beyond Colliders at CERN: Beyond the Standard Model Working Group Report,” *J. Phys. G* **47** (2020) no. 1, 010501, [arXiv:1901.09966 \[hep-ex\]](#).
- [30] M. Bauer, M. Neubert, S. Renner, M. Schnubel, and A. Thamm, “The Low-Energy Effective Theory of Axions and ALPs,” *JHEP* **04** (2021) 063, [arXiv:2012.12272 \[hep-ph\]](#).
- [31] M. Bauer, M. Neubert, S. Renner, M. Schnubel, and A. Thamm, “Flavor probes of axion-like particles,” *JHEP* **09** (2022) 056, [arXiv:2110.10698 \[hep-ph\]](#).
- [32] D. Aloni, Y. Soreq, and M. Williams, “Coupling QCD-Scale Axionlike Particles to Gluons,” *Phys. Rev. Lett.* **123** (2019) no. 3, 031803, [arXiv:1811.03474 \[hep-ph\]](#).
- [33] G. Dalla Valle Garcia, F. Kahlhoefer, M. Ovchinnikov, and A. Zaporozhchenko, “Phenomenology of axionlike particles

- with universal fermion couplings revisited,” *Phys. Rev. D* **109** (2024) no. 5, 055042, [arXiv:2310.03524 \[hep-ph\]](#).
- [34] P. Ilten, Y. Soreq, M. Williams, and W. Xue, “Serendipity in dark photon searches,” *JHEP* **06** (2018) 004, [arXiv:1801.04847 \[hep-ph\]](#).
- [35] K. Bondarenko, A. Boyarsky, D. Gorbunov, and O. Ruchayskiy, “Phenomenology of GeV-scale Heavy Neutral Leptons,” *JHEP* **11** (2018) 032, [arXiv:1805.08567 \[hep-ph\]](#).
- [36] M. H. Reno and D. Seckel, “Primordial Nucleosynthesis: The Effects of Injecting Hadrons,” *Phys. Rev. D* **37** (1988) 3441.
- [37] M. Pospelov and J. Pradler, “Metastable GeV-scale particles as a solution to the cosmological lithium problem,” *Phys. Rev. D* **82** (2010) 103514, [arXiv:1006.4172 \[hep-ph\]](#).
- [38] G. B. Gelmini, M. Kawasaki, A. Kusenko, K. Murai, and V. Takhistov, “Big Bang Nucleosynthesis constraints on sterile neutrino and lepton asymmetry of the Universe,” *JCAP* **09** (2020) 051, [arXiv:2005.06721 \[hep-ph\]](#).
- [39] M. Kawasaki, K. Kohri, and T. Moroi, “Big-Bang nucleosynthesis and hadronic decay of long-lived massive particles,” *Phys. Rev. D* **71** (2005) 083502, [arXiv:astro-ph/0408426](#).
- [40] **Particle Data Group** Collaboration, R. L. Workman *et al.*, “Review of Particle Physics,” *PTEP* **2022** (2022) 083C01.
- [41] K. Akita and M. Yamaguchi, “A precision calculation of relic neutrino decoupling,” *JCAP* **08** (2020) 012, [arXiv:2005.07047 \[hep-ph\]](#).
- [42] K. Akita, G. Baur, M. Ovchinnikov, T. Schwetz, and V. Syvolap, “Impact of new physics on neutrinos: case of particles do not directly decaying into neutrinos,” (to appear), [arXiv:2024.XXXXX \[hep-ph\]](#).
- [43] **Planck** Collaboration, N. Aghanim *et al.*, “Planck 2018 results. VI. Cosmological parameters,” *Astron. Astrophys.* **641** (2020) A6, [arXiv:1807.06209 \[astro-ph.CO\]](#). [Erratum: *Astron. Astrophys.* 652, C4 (2021)].
- [44] G. Mangano, G. Miele, S. Pastor, and M. Peloso, “A Precision calculation of the effective number of cosmological neutrinos,” *Phys. Lett. B* **534** (2002) 8–16, [arXiv:astro-ph/0111408](#).
- [45] J. J. Bennett, G. Buldgen, M. Drewes, and Y. Y. Y. Wong, “Towards a precision calculation of the effective number of neutrinos N_{eff} in the Standard Model I: the QED equation of state,” *JCAP* **03** (2020) 003, [arXiv:1911.04504 \[hep-ph\]](#). [Addendum: *JCAP* 03, A01 (2021)].
- [46] J. J. Bennett, G. Buldgen, P. F. De Salas, M. Drewes, S. Gariazzo, S. Pastor, and Y. Y. Y. Wong, “Towards a precision calculation of N_{eff} in the Standard Model II: Neutrino decoupling in the presence of flavour oscillations and finite-temperature QED,” *JCAP* **04** (2021) 073, [arXiv:2012.02726 \[hep-ph\]](#).
- [47] J. Froustey, C. Pitrou, and M. C. Volpe, “Neutrino decoupling including flavour oscillations and primordial nucleosynthesis,” *JCAP* **12** (2020) 015, [arXiv:2008.01074 \[hep-ph\]](#).
- [48] M. Cielo, M. Escudero, G. Mangano, and O. Pisanti, “Neff in the Standard Model at NLO is 3.043,” *Phys. Rev. D* **108** (2023) no. 12, L121301, [arXiv:2306.05460 \[hep-ph\]](#).
- [49] G. Jackson and M. Laine, “QED corrections to the thermal neutrino interaction rate,” *JHEP* **05** (2024) 089, [arXiv:2312.07015 \[hep-ph\]](#).
- [50] M. Drewes, Y. Georis, M. Klasen, L. P. Wiggering, and Y. Y. Y. Wong, “Towards a precision calculation of N_{eff} in the Standard Model III: Improved estimate of NLO corrections to the collision integral,” [arXiv:2402.18481 \[hep-ph\]](#).
- [51] S. Hannestad and J. Madsen, “Neutrino decoupling in the early universe,” *Phys. Rev. D* **52** (1995) 1764–1769, [arXiv:astro-ph/9506015](#).
- [52] **Simons Observatory** Collaboration, P. Ade *et al.*, “The Simons Observatory: Science goals and forecasts,” *JCAP* **02** (2019) 056, [arXiv:1808.07445 \[astro-ph.CO\]](#).
- [53] **Planck** Collaboration, N. Aghanim *et al.*, “Planck 2018 results. I. Overview and the cosmological legacy of Planck,” *Astron. Astrophys.* **641** (2020) A1, [arXiv:1807.06205 \[astro-ph.CO\]](#).
- [54] M. Ovchinnikov, J.-L. Tastet, O. Mikulenko, and K. Bondarenko, “Sensitivities to feebly interacting particles: Public and unified calculations,” *Phys. Rev. D* **108** (2023) no. 7, 075028, [arXiv:2305.13383 \[hep-ph\]](#).
- [55] C. Bierlich *et al.*, “A comprehensive guide to the physics and usage of PYTHIA 8.3,” *SciPost Phys. Codeb.* **2022** (2022) 8, [arXiv:2203.11601 \[hep-ph\]](#).